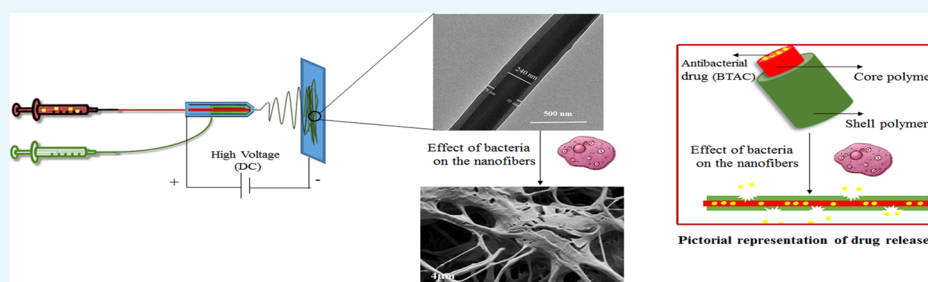


# Bacteria-Responsive Single and Core–Shell Nanofibrous Membranes Based on Polycaprolactone/Poly(ethylene succinate) for On-Demand Release of Biocides

Zahra Abdali,<sup>†,‡</sup> Sarvesh Logsetty,<sup>‡</sup> and Song Liu<sup>\*,†,§,||</sup>

<sup>†</sup>Biomedical Engineering, Faculty of Engineering, <sup>‡</sup>Director of Manitoba Firefighters Burn Unit, Professor in the Departments of Surgery and Psychiatry, Rady Faculty of Health Sciences, <sup>§</sup>Department of Biosystems Engineering, and <sup>||</sup>Department of Medical Microbiology, University of Manitoba, Winnipeg R3T 2N2, Canada

## S Supporting Information



**ABSTRACT:** Traditional antibacterial dressings continuously elute biocides, even if there are no bacteria. This unneeded release can cause cytotoxicity, increase costs, and delay healing. We designed a bacteria-responsive nanofibrous wound dressing, which can be degraded in the presence of bacteria to release antimicrobial agents. A model biocide, benzyl dimethyl tetradecyl ammonium chloride (BTAC), was incorporated into bacteria-degradable polymers [polycaprolactone and poly(ethylene succinate)] in two ways: evenly distributed inside the polymers as single nanofibers and encapsulated in a core surrounded by the same polymers as core–shell nanofibers. Because of bacterial activity (both lipase secretion and acidic pH), degradation of the fibers was facilitated and caused the release of incorporated BTAC. BTAC-loaded single and core–shell nanofibers presented >1 log reduction of both *Staphylococcus aureus* and *Escherichia coli* within 2 h. Additionally, the core–shell structure provided a more controlled release of BTAC with prolonged antibacterial properties than single nanofibers. The core–shell nanofibers also exhibited minimal cytotoxicity against human fibroblast cells (>80% viable cells after 24 h contact). These nanofibrous mats have the potential to selectively release antibacterial agents to prevent wound infections without delaying wound healing.

## 1. INTRODUCTION

Chronic wounds are a global healthcare issue, especially in the context of increasing prevalence of chronic conditions such as high blood pressure, diabetes, and obesity. Wound care dressings play an important role in the healing process of chronic wounds. Antibacterial agents have been incorporated into wound dressings to eliminate colonization and treat bacterial infections in the wound.<sup>1</sup> The traditional design of biocide release systems has been based on the continuous release of antibacterial agents, even if there are no bacteria present. This unneeded release of antibacterial agents can cause undesirable cytotoxicity to skin cells, which can delay wound healing. Additionally, the system could be depleted of its antibacterial agent in its reservoir before real infections occur.

To reduce the misuse and overuse of antibacterial agents, bacteria-responsive delivery of biocides has been suggested. Bacteria secrete various virulence factors, which can act as triggering factors for the system.<sup>2,3</sup> As a result, the system will release the antimicrobial payload only when and where there is

an interaction with bacteria. Bacterial enzymes are one of the most common virulence factors that researchers have used as a triggering factor in bacteria-responsive systems.<sup>4–6</sup> In the study by Bean et al.,<sup>6</sup> hyaluronidase secreted by *Staphylococcus aureus* was utilized for the responsive release of bacteriophage K embedded in a photocross-linkable hyaluronic acid-based hydrogel. In another bacteria-responsive system designed by Craig et al.,<sup>4</sup> *S. aureus* protease stimulated the degradation of polypeptide-based drug-loaded nanoparticles. There are limitations in each of these studies: hyaluronidase is mostly secreted by Gram-positive bacteria with little to no excretion in Gram-negative bacteria, and protease is naturally present in the extracellular matrix and is also secreted by host cells. In contrast, lipase is secreted by both Gram-positive and Gram-negative bacteria and is mostly the product of bacteria.

Received: November 9, 2018

Accepted: February 11, 2019

Published: February 22, 2019

Lipase-labile bonds, such as fatty acid esters or anhydrides, can be degraded in response to lipase. Polycaprolactone (PCL) is a biodegradable polyester with a relatively slow degradation rate.<sup>7</sup> There are few studies about using PCL in bacteria-triggered systems. Xiong et al.<sup>8</sup> designed a lipase-sensitive triple-layered nanogel (TLN) as a nanocarrier. In this approach, the TLN contained a PCL interlayer between the cross-linked polyphosphoester core and the shell of poly(ethylene glycol). The PCL fence of the TLN was subjected to degradation by the activity of bacterial lipases.

One important factor that should be considered in the design of a bacteria-responsive system is the rate of response. An ideal bacteria-responsive system should quickly respond to triggering factors secreted by bacteria. The rate of response is dependent on both the physical and chemical structures of the system. Systems with high specific surface area such as nanoparticles and nanofibers have a good chance to be triggered and provide a fast response. Besides high specific surface area, electrospun polymeric nanofibers are highly compliant and have high porosity with excellent pore interconnectivity. These features allow them to have intimate contact with the wound bed despite highly variable and irregular wound shape and also transport extra body fluid from the wound to decrease the chance of infection.<sup>9–12</sup> Over the last two decades, PCL, a biodegradable synthetic polymer, has emerged as a class of biomaterials of growing interest. Although PCL has shown excellent biocompatibility and efficacy both in vitro and in vivo, its highly hydrophobic nature and slow degradation may hinder its use as bacteria-responsive wound dressings.<sup>13</sup> To overcome this limitation, we proposed to blend PCL with another biodegradable polymer. Poly(ethylene succinate) (PES) is an aliphatic biodegradable polyester, which has a higher rate of degradation than PCL.<sup>14</sup> In this study, we intended to prepare electrospun nanofibrous mats based on PCL and PES, leading to an improved degradation in response to bacteria. To the best of our knowledge, this is the first report of bacteria-responsive electrospun core–shell nanofibers based on PCL/PES. It is worthwhile to mention that in the single electrospinning process, the drug added in the polymer solution can quickly migrate to the surface or near the surface of the nanofibers together with the evaporating solvent, leading to a high percentage of initial burst release of the loaded drugs and lack of control over the release.<sup>15</sup> This significant drawback can be avoided through the use of core–shell nanofibers fabricated through coaxial electrospinning.<sup>15,16</sup> In this method, two polymer solutions are pushed through two concentrically arranged orifices of a spinneret. As the solutions are pumped out of the spinneret, the outer polymer covers the inner “core” material. As a result, the deposited polymer nanofibers will have a core–shell structure.<sup>17</sup> Drug encapsulation in the core could lead to drug release in a well-controlled manner and prolonged antimicrobial efficacy.<sup>18</sup> On the basis of the above-mentioned rationale, we intended to prepare core–shell nanofibers, which consist of PCL/PES as the shell and a model biocide benzyl dimethyl tetradecyl ammonium chloride (BTAC) blended in poly(vinylpyrrolidone) (PVP) as the core. The morphology, diameter, and the core–shell structure of nanofibers were studied using scanning electron microscopy (SEM) and transmission electron microscopy (TEM). These nanofibrous mats can be degraded when incubated in the suspension of *Escherichia coli* or *S. aureus*. Drug release and antibacterial efficacy of single and core–shell nanofibers were

compared, respectively. Finally, the cytotoxicity of nanofibers was evaluated using the (3-[4, 5-dimethylthiazol-2-yl]-2, 5-diphenyltetrazolium bromide) (MTT) assay.

## 2. RESULTS AND DISCUSSION

PCL and PES polymers were used as the shell polymers in the fabrication of core–shell nanofibers because of their bacteria-responsive properties. PVP is a biocompatible and water-soluble polymer, which could be easily dissolved in contact with aqueous media. PVP was added in antibacterial solution as one of the components in the core to improve the electrospinnability of the core solution (Figure 1).

**2.1. Morphology of Electrospun Nanofibers.** A total of 8% PCL solution and 20% PES solution were mixed at various

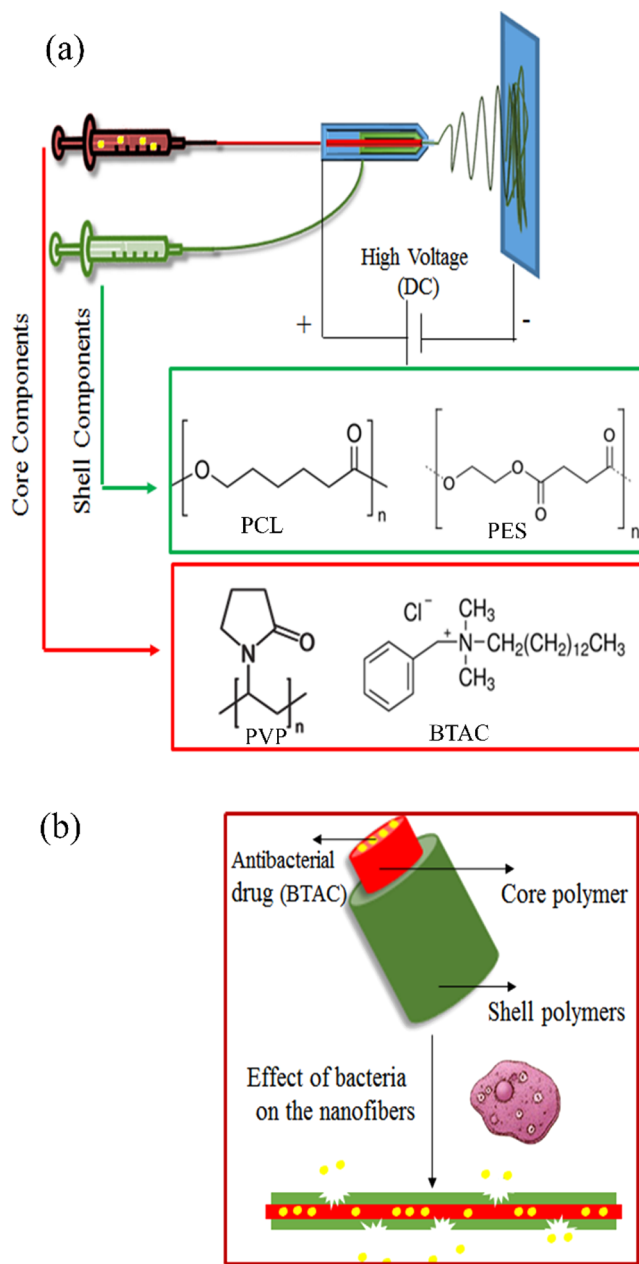


**Figure 1.** (a) Coaxial electrospinning of two immiscible polymer solutions and (b) pictorial representation of core–shell nanofiber degradation and drug release.

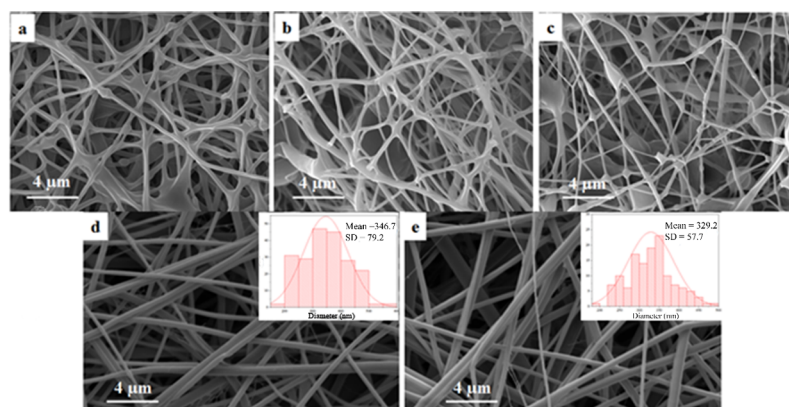


**Figure 2.** Morphology of nanofibers: (a) PCL/PES 5:1, (b) PCL/PES 2:1, (c) PCL/PES 1:1, (d) core-shell 8% PCL/30% PES 1:1/15% PVP with 2.5% BTAC, and (e) single 8% PCL/30% PES 1:1 with 2.5% BTAC.

ratios and used for electrospinning. After the fabrication of single and core-shell electrospun mats, we studied their morphology (Figure 2). Nanofibers electrospun with various PCL/PES ratios all showed the merged morphology, especially PCL/PES 1:1 (Figure 2c), with the highest ratio of PES among all samples. Because of the relatively lower molecular weight of PES than that of PCL, the polymer solution with a higher amount of PES resulted in lower spinability and more beads.

Increasing the concentration of PES from 20 to 30% caused a significant change in the morphology of nanofibers. As could be seen in Figure 2d,e, the morphology of core-shell and single nanofibers changed from bead-on-string to a smooth complete fibrous structure. The 1:1 ratio for PCL/PES is more preferable than other ratios because of higher degradability of PES than PCL. Therefore, the concentration (30% PES) and ratio (1:1 PCL/PES) were kept in all the following experiments. Both single and core-shell drug-loaded nanofibers had nanosized averaged diameters of 329 and 346 nm, respectively.

The coaxially electrospun nanofibers were further characterized by TEM. Because the core polymer PVP is more electron-dense than the shell polymers PCL and PES, the core and shell components should present a good contrast under TEM.<sup>19</sup> TEM micrographs of drug-loaded nanofibers (shell: PCL/PES and core: PVP/2.5% BTAC) were taken and are presented in Figure 3. The micrographs clearly showed the core-shell structure of the coaxially electrospun nanofiber. A sharp boundary between the shell and core along the length of the fiber was present, indicating successful formation of the desired core-shell structure. It has been explained in the study by Sun et al.<sup>20</sup> that during coaxial electrospinning, the time of

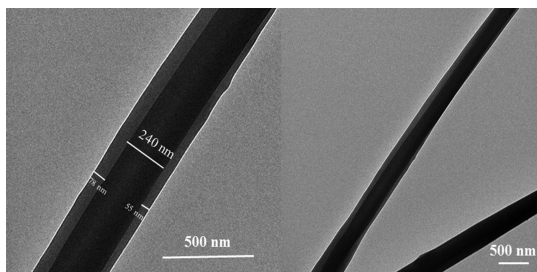


**Figure 3.** TEM micrographs of the drug-loaded core-shell nanofiber (shell: PCL/PES, core: PVP, 2.5% BTAC).

the bending instability is much shorter than that of diffusion spreading so that the sharp boundary could survive.

**2.2. Drug Release Profile.** To check the responsive nature of the fabricated nanofibrous membranes, they were immersed in bacterial supernatant and tryptone soya broth (TSB). Released BTAC was allowed to form a complex with orange II dye via electrostatic interaction, extracted with chloroform, and then quantified using spectrophotometry. As can be seen from Figure 4, the percent of BTAC release within 24 h from the

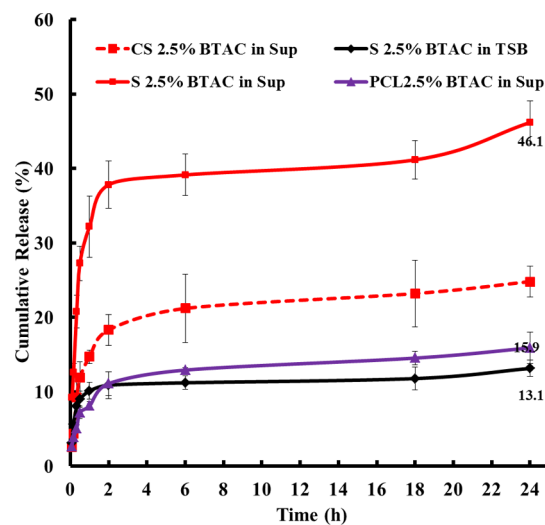


**Figure 4.** Cumulative release of BTAC from the single and core-shell nanofibers (sup: bacterial supernatant and TSB).

single electrospun nanofibrous membrane S 2.5% BTAC (the sample code is defined in Table 1) in TSB (13.1%) is much lower than that in *S. aureus* culture supernatant (46.1%) ( $P$ -value: 0.0001). This demonstrated the bacteria-responsive release of BTAC from the nanofibrous membrane. PCL 2.5% BTAC referred to the BTAC-loaded PCL nanofiber, whereas S 2.5% BTAC was fabricated through blending PCL and PES with a 1:1 blend ratio. Comparison of the cumulative release between PCL 2.5% BTAC (15.9%) and S 2.5% BTAC (46.1%) in the supernatant showed the role of PES in the bacteria-responsive degradation of nanofibers. This confirms that PES is more sensitive to bacterial degradation.

It is worth mentioning that all the core-shell nanofibers displayed lower percent of BTAC release in TSB than single

**Table 1. Feed Composition of Fabricated Nanofibers**

sample code	feed composition
PCL/PES 5:1	
PCL/PES 2:1	PCL 8% + PES 20%
PCL/PES 1:1	
PCL 2.5% BTAC	single electrospinning: PCL 8% + 2.5% BTAC
S 2.5% BTAC	single electrospinning: PCL 8% + PES 30%
S 4.5% BTAC	(blending 1:1) + 2.5 and 4.5% BTAC
CS 2.5% BTAC	coaxial electrospinning:
CS 3.5% BTAC	shell/PCL 8% + PES 30% (blending 1:1)
CS 4.5% BTAC	core/PVP 15% + 2.5, 3.5, and 4.5% BTAC

equivalents in the first 30 min (Figure S1). It showed that the core–shell nanofibers present a better bacteria responsiveness and lower burst release of the payload. In single nanofibers, BTAC was directly dispersed into the polymer solution. During the electrospinning process, BTAC migrated to the surface or near the surface of the fibers together with the evaporating solvent and contributed to the relatively high release of the payload in the absence of a bacterial supernatant. BTAC was better encapsulated in the core–shell fibers, and its release was dependent on both degradation of the shell in presence of bacterial enzyme and dissolution of the core matrix polymer PVP. The better responsiveness and more controllable payload release in the case of core–shell nanofibers could minimize unnecessary side effects of the encapsulated drug. Also, in a bacterial supernatant, CS 2.5% BTAC displayed lower burst release in the first 2 h (18.3%, Figure 4) than S 2.5% BTAC (37.8%, Figure 4) in the bacterial supernatant. This slower depletion of BTAC may potentially lead to an extended period of antibacterial efficacy from the BTAC-loaded core–shell nanofiber.<sup>21</sup>

To better understand the effect of PES on the degradation, we immersed nanofibers in TSB and bacterial supernatant of *S. aureus* (ATCC 29213) for 72 h and studied those samples using SEM. As can be seen from Figure 5, all tested samples including PCL single electrospun nanofibers, PCL/PES single electrospun nanofibers, and PCL/PES core–shell electrospun nanofibers appeared to be stable in TSB. Different degradabilities of PCL single electrospun nanofibers and PCL/PES single electrospun nanofibers could be observed in Figure 5a,b. Nanofibers containing PES showed higher disintegration than PCL after immersion in the bacterial supernatant for 72 h. Bacterial activity caused enzymatic degradation of ester linkage in PES nanofibers. This observation is consistent with the study of Hoang et al.,<sup>14</sup> which shows the comparison of the enzymatic biodegradation of PES, PCL, and poly(3-hydroxybutyrate) (PHB) in the form of films. The PES film showed a rough surface with small cracks after 2 days of incubation in the culture of actinomycete strain HS 45-1. PHB and PCL films were degraded within 6 days with a lower rate of degradation than PES. These results also correlate with the release data in Figure 4. The higher degradation rate of PES than PCL led to higher 24 h release of BTAC from S 2.5% than PCL 2.5% in the bacterial supernatant.

The acidic pH of the bacterial supernatant (pH = 5) could be another factor that facilitates the degradation of the nanofibers. To test this hypothesis, we also measured the percentage of cumulative release of S 2.5% BTAC in the pH = 5 buffer within 1 h ( $12.1 \pm 0.4\%$ ), which was significantly

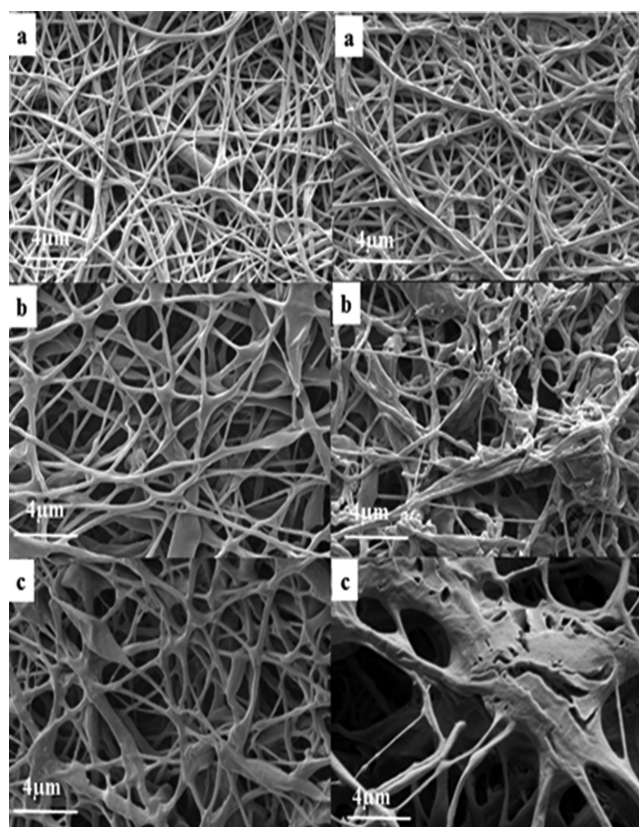


**Figure 5.** Morphology of nanofibers after being immersed in TSB (left) and supernatant (right) for 72 h: (a) PCL, (b) S/PCL/PES, and (c) CS/PCL/PES.

higher than in TSB ( $10.1 \pm 0.4\%$ ) but lower than in the bacterial supernatant (more than two times lower). Acute wounds have a neutral pH and, during acute wound healing, there is a drop in pH caused by various factors, including hypoxia and increased production of lactic acid.<sup>22</sup> Therefore, it can be concluded that both lipase enzyme and acidic pH play a role in the degradation of nanofibers, although the effect of lipase enzyme is more significant.

**2.3. Antibacterial Activity.** The aim of the present study was to design an antimicrobial and biocompatible wound dressing. Among different possibilities, BTAC, a quaternary ammonium compound (QAC), was chosen in the present work. QACs are well-known as effective biocides against various microorganisms including bacteria.<sup>23,24</sup> QACs show a detergent-like mechanism of antimicrobial action, which is due to their amphiphilic nature. QACs' long alkyl side chains could permeate into the intramembrane region of the bacterial membrane and lead to the leakage of cytoplasmic materials and cell lysis. This invasion is due to strong electrostatic interaction between the positively charged QAC head and the negatively charged bacterial membrane.<sup>23</sup> As our system was designed to tackle the infections caused by two common strains of bacteria *S. aureus* and *E. coli*, we conducted antibacterial test against these two bacteria. Similar to *S. aureus*, *E. coli* also possesses lipase activity.<sup>25</sup>

Tables 2 and 3 show the antibacterial efficacy of the BTAC-loaded nanofibers against *S. aureus* and *E. coli* at around 8 log cfu/mL concentration. Bacterial reduction caused by the nanofibers progressively increased as the contact time increased and the nanofibers loaded with higher percentages

**Table 2. Antibacterial Activity of Nanofibers with Different Formulations against *S. aureus*<sup>a</sup>**

electrospun samples	bacterial reduction (%) at various contact time (min)					
	5	10	20	30	60	120
CS 2.5% BTAC	45.7 ± 3.7	61.6 ± 4.7		82.8 ± 3.9	96.1 ± 1.0	97.9 ± 0.3
S 2.5% BTAC	67.3 ± 8.5	88.7 ± 1.7		94.6 ± 3.0	97.6 ± 0.8	100
CS 3.5% BTAC	78.4 ± 6.9	88.3 ± 1.5		99.5 ± 0.5	99.9 ± 0.1	100
S 3.5% BTAC	75.3 ± 1.3	90.7 ± 0.8	99.5 ± 0.8	99.7 ± 0.4	100	100
CS 4.5% BTAC	99.6 ± 0.3	100				
S 4.5% BTAC	100					
PCL 2.5% BTAC	34.4 ± 6.6	47.7 ± 6.8	50.4 ± 4.0	58.0 ± 2.9	65.5 ± 6.6	83.9 ± 1.3
BTAC	96.1 ± 0.2	98.5 ± 0.9	100			

<sup>a</sup>Inoculum concentration of *S. aureus* was  $6.3 \times 10^8$  cfu mL<sup>-1</sup>.

**Table 3. Antibacterial Activity of Nanofibers with Different Formulations against *E. coli*<sup>a</sup>**

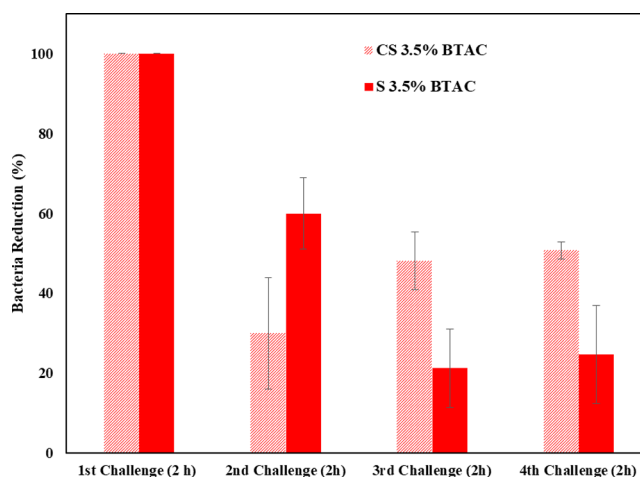
electrospun samples	bacterial reduction (%) at various contact time (min)					
	5	10	20	30	60	120
CS 2.5% BTAC	7.9 ± 0.9	15.5 ± 3.1		53.0 ± 5.2	60.3 ± 5.2	96.9 ± 0.5
S 2.5% BTAC	14.9 ± 3.8	26.3 ± 3.1		74.0 ± 2.0	78.6 ± 3.6	98.9 ± 0.4
CS 3.5% BTAC	27.2 ± 1.4	37.1 ± 1.82		94.8 ± 0.5	95.2 ± 0.4	100
S 3.5% BTAC	38.9 ± 3.8	49.1 ± 3.1	61.6 ± 4.2	96.3 ± 0.6	97.1 ± 0.4	100
CS 4.5% BTAC	45.9 ± 0.9	60.8 ± 3.5	70.2 ± 1.7	97.0 ± 0.3	99.3 ± 0.2	100
S 4.5% BTAC	57.3 ± 4.3	64.9 ± 2.3	76.6 ± 3.0	97.8 ± 0.1	100	100
PCL 2.5% BTAC	5.7 ± 2.9	12.0 ± 1.8	24.0 ± 4.6	38.3 ± 6.8	48.7 ± 5.6	47.8 ± 3.2
BTAC	95.3 ± 0.3	96.0 ± 0.2	98.8 ± 0.5	100		

<sup>a</sup>Inoculum concentration of *E. coli* was  $7.9 \times 10^8$  cfu mL<sup>-1</sup>.

of BTAC presented faster inactivation of bacteria. As expected, all the core–shell nanofibers showed slower bacteria inhibition than single nanofibers, which is consistent with the release data. The hydrophobic nature of the shell (PCL and PES) could effectively retard the penetration of water into the fibers and release of BTAC was dependent on the degradation of the shell polymers in the bacterial supernatant.<sup>15</sup> The BTAC-loaded nanofibers appeared to be more effective against *S. aureus* as a Gram-positive bacterium than the Gram-negative bacterium *E. coli*. This is likely related to the outer membrane in Gram-negative bacteria. QACs target bacterial cell membranes. Gram-negative bacteria are encapsulated by two cellular membranes and a thin layer of peptidoglycan. Because of the presence of this second membrane (outer membrane), they are better protected against QACs.<sup>23</sup> Our result was consistent with the study of Liu et al.,<sup>24</sup> which also showed the lower sensitivity of Gram-negative bacteria than to QACs' Gram-positive ones.

We also tested the antibacterial property of free BTAC and compared it with the results of BTAC-loaded nanofibers. The concentration of free BTAC was set to be equivalent to the cumulative release of S 3.5% BTAC within 2 h. S 3.5% BTAC obtained 100% reduction of *S. aureus* and *E. coli* within 60 and 120 min, respectively. However, faster bacteria killing activity was observed for free BTAC against both bacteria. Free BTAC obtained 100% reduction of both tested bacteria before 60 min. Although free biocide was fast in inactivating bacteria, we cannot expect prolonged and efficient antibacterial properties in the wound because free biocide can be easily washed out by wound exudate. In addition, the sample PCL 2.5% BTAC showed significantly lower percent reduction of bacteria than S 2.5% BTAC (*P*-value: 0.01). This was due to the absence of PES in the shell and therefore slow biodegradation of the shell polymer as discussed in the drug release section.

The release study clearly showed the slower release of BTAC from core–shell nanofibers than single ones. To better perceive its effect on prolonged antibacterial properties, we conducted the repeated antibacterial experiment. It can be seen in Figure 6 that in the second trial, the antibacterial efficacy of

**Figure 6. Repeated antibacterial test against *S. aureus*.**

S 3.5% BTAC is still higher than that of CS 3.5% BTAC. However, in the third and fourth antibacterial tests, CS 3.5% BTAC showed higher bacterial reduction. In this experiment, we discarded the BTAC released in the previous challenge and moved the mats to a fresh bacterial suspension. If we consider the effect of drug cumulatively released in each challenge, a higher percentage of bacterial reduction would be observed (higher than 50% in the 4th challenge in the case of CS 3.5% BTAC).

**2.4. Cytotoxicity Test.** An ideal wound dressing should not exert severe cytotoxicity to skin cells, which could be evaluated through *in vitro* cytotoxicity tests.<sup>26–28</sup> One of the most important advantages of bacteria-triggered systems is to reduce any unnecessary cytotoxicity toward skin cells through on-demand release of antibacterial drugs. In the previous section, we analyzed the antibacterial efficacy of the BTAC-loaded nanofibers. To have an insight about cell viability of the nanofibers, human dermal fibroblast cells were exposed to the nanofibrous membranes. MTT results for all the mats after 24 h contact with fibroblast cells are presented in Figure 7.

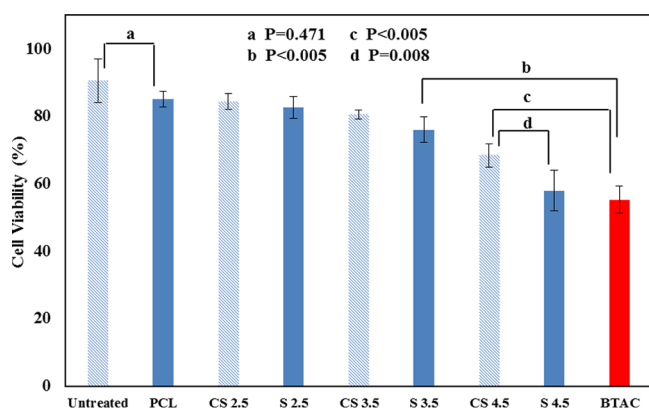


**Figure 7.** Cell viability of nanofibers within 24 h contact. Note: Untreated refers to the core–shell nanofiber with no drug in the core; % BTAC is omitted in all the sample codes to save space in the bar graph.

Untreated nanofibers (CS nanofibers with no drug in the core) showed the highest cell viability. There is no significant difference between cell viability of untreated and PCL single nanofibers ( $P = 0.471$ ), which indicated low release of BTAC from PCL single nanofibers in the fibroblast culture. CS 2.5% BTAC and S 2.5% BTAC presented >96% reduction of both *S. aureus* and *E. coli* within 2 h of contact. However, >82% fibroblast cells were still viable after 24 h incubation with both samples and not significantly different from the nanofiber without BTAC, confirming the bacteria-responsive nature of these samples. There were no significant differences between cell viability of single and core–shell nanofibers loaded with 2.5 or 3.5% BTAC. However, at higher concentration of BTAC (4.5%), we observed a significant difference in cell viability between single (S 4.5% BTAC) and core–shell nanofibers (CS 4.5% BTAC) ( $P = 0.008$ ).

To compare the cell viability of BTAC-loaded nanofibers and free BTAC, we also included unencapsulated BTAC in the MTT assay. As nanofibers were in contact with fibroblast cells for 24 h, the concentration of BTAC for the MTT assay was chosen to be equivalent to the cumulative release of BTAC from S 3.5% BTAC within 24 h (34 mg/L). According to Figure 7, BTAC damaged almost half of fibroblast cells ( $55.2 \pm 4.0\%$  viable cells). The low cell viability caused by free BTAC indicates the nonselective nature of BTAC. The cell viability of free BTAC was significantly lower than that of S 3.5% BTAC and even CS 4.5% BTAC. Both S 3.5% BTAC and CS 4.5% BTAC could achieve total reduction of the two tested bacteria within 2 h of contact (Tables 2 and 3). These results highlight the benefit of the responsive release of biocides: avoiding unnecessary cytotoxicity toward mammalian cells. CS 3.5% BTAC could be considered as a potential candidate in clinical

application as an antibacterial wound dressing for chronic wounds in view of its low cytotoxicity toward fibroblasts and highly effective antibacterial activity toward *S. aureus* and *E. coli*.

According to the cell vitality results, it can be concluded that BTAC released in the cell media (even in the 24 h) is not at the cytotoxic level. We also measured the release of BTAC from S 2.5% BTAC in the fibroblast supernatant within 1 h. As expected, the percentage of release of BTAC in the fibroblast supernatant ( $11.3 \pm 0.5\%$ ) was significantly lower than that in the bacterial supernatant ( $32.2 \pm 0.8\%$ ) ( $P = 0.0001$ ). Clearly, the drug-loaded nanofibrous mats demonstrated selective responsiveness to bacteria.

### 3. CONCLUSIONS

Because of exceptional properties of bacteria-responsive systems, we fabricated core–shell nanofibers whose shell polymers could be degraded in response to bacteria and therefore present on-demand release of the model biocide (BTAC) encapsulated in the core. This smart system showed significantly higher biocide release when it was in contact with the bacterial supernatant than in TSB. More controllable release of BTAC from core–shell nanofibers than single ones could provide a prolonged efficient antibacterial activity. Besides, because of on-demand release of the biocidal payload from the nanofibers, they showed much lower cytotoxicity against human fibroblast cells than the free biocide. The efficient antibacterial activity of these core–shell nanofibers with no severe cytotoxicity makes them potential candidates for tackling wound infections.

### 4. MATERIALS AND METHODS

**4.1. Materials.** PCL (MW = 80 000 g mol<sup>-1</sup>), PES (MW = 10 000 g mol<sup>-1</sup>), PVP 40 000 MW, dimethylformamide (DMF), dichloromethane (DCM), BTAC, MTT, dimethyl sulfoxide (DMSO), and orange II sodium salt were purchased from Sigma. Inovenso electrospinning apparatus (model Ne300, Turkey) was used to fabricate single and core–shell nanofibers. American Type Culture Collection (ATCC) strains were used in the antibacterial test, including *S. aureus* ATCC 29213 and *E. coli* ATCC 25922. ATCC-PCS-201 neonatal human dermal fibroblast was purchased from Cedarlane Corporation, Canada.

**4.2. Fabrication of Nanofibers.** PCL and PES were dissolved in DCM/DMF (4:1) at a concentration of 8 and 20 wt %, respectively. PCL solution (8 wt %) was mixed with PES solution (20 wt %) in volume ratios of (PCL/PES) 5:1, 2:1, and 1:1. Then, the mixed solutions were used in single electrospinning experiments. Voltage (20 kV), flow rate of solution (1 mL/h), and distance between syringe and collector (18 cm) were set for each sample.

For core–shell electrospinning, PVP was adopted as the core component and DCM/DMF (4:1) solution of PCL/PES was used as the shell component. PVP was dissolved in DCM/DMF (4:1) at the concentration of 15 wt %. Flow rates of core and shell solution were 0.3 and 1 mL/h, respectively.

To prepare drug-loaded nanofibers, BTAC was dissolved in DCM and added to PCL/PES blend for single nanofibers or to PVP for core–shell nanofibers. BTAC (2.5, 3.5, or 4.5%) with respect to the weight of the whole polymer was used in the fabrication of antibacterial nanofibers. The sample codes are listed in Table 1.

**4.3. Morphology of Nanofibers.** The morphology and diameter of nanofibers were thoroughly studied using SEM (FEI Nova NanoSEM 450). To visualize the effect of bacterial activity on degradation of nanofibers, we immersed them in a bacterial supernatant solution or TSB for 72 h and observed them under a scanning electron microscope. An 18 h bacterial culture ( $10^8$  colony-forming units (cfu)  $\text{mL}^{-1}$  *S. aureus*) was used to prepare the supernatant. To prepare the supernatant, we first centrifuged the 18 h culture (5000 rpm for 15 min) and then filter-sterilized ( $0.22 \mu\text{m}$  filters) it before storage at  $4^\circ\text{C}$ .

The core-shell structure of the prepared nanofibers was characterized by TEM (JEOL JEM-2100F) at an accelerating voltage of 200 kV, for which carbon-coated copper grids were used to collect the nanofibers.

**4.4. Drug Release Measurement.** To study the drug release, nanofibers were immersed in either the supernatant of *S. aureus* culture or TSB (4 mg in 2 mL media) and incubated at  $37^\circ\text{C}$ . To obtain the cumulative release of BTAC, 600  $\mu\text{L}$  of eluted drug medium was removed for quantification and replenished with 600  $\mu\text{L}$  fresh release medium to maintain a sink condition. Removed medium was mixed with a 0.25 mL orange II dye solution (Figure 8). After 5 min, 600  $\mu\text{L}$  of

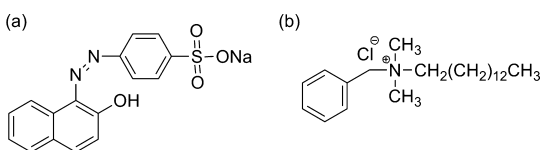


**Figure 8.** Structures of (a) orange II dye and (b) BTAC.

chloroform was added to the dye-BTAC complex, and the mixture was vortexed for 45 s to ensure that chloroform and the dye solution were mixed thoroughly. A 600  $\mu\text{L}$  of the chloroform phase (the bottom layer) was removed into a cuvette, and the absorbance was measured at 485 nm to allow quantification of the dye-BTAC complex and hence BTAC.

**4.5. Antibacterial Test.** The antibacterial activity of the nanofiber mats was tested by a colony-counting method<sup>24</sup> against *S. aureus* ATCC 29213 and *E. coli* ATCC 25922, which are commonly found in burn wounds, and representatives of Gram-positive and Gram-negative bacteria, respectively. For the antibacterial studies, logarithmic-phase cultures were prepared by initially suspending several colonies in phosphate-buffered saline (PBS, 0.1 M, pH 7.4) at a density equivalent to a 0.5 McFarland standard of  $1 \times 10^8$  cfu  $\text{mL}^{-1}$  and then diluted 100 times to  $1 \times 10^6$  cfu  $\text{mL}^{-1}$ . A 15  $\mu\text{L}$  of the diluted *E. coli* or *S. aureus* suspension was further diluted into 45 mL cation-supplemented Mueller-Hinton broth or TSB. After overnight incubation at  $37^\circ\text{C}$ , the concentration of bacteria went up to  $10^8$  cfu  $\text{mL}^{-1}$ .

A 2 mL of such bacteria suspension was added to a 4 mg nanofibrous membrane and incubated. At the predetermined contact times, 150  $\mu\text{L}$  of the bacteria culture was taken from the flask, neutralized, and serially diluted with PBS. A 30  $\mu\text{L}$  of the diluted sample was then spread onto a tryptone soya agar plate (CM 0131, OXOID). After incubation of the plates at  $37^\circ\text{C}$  for 18 h, the number of viable bacteria (colonies) was counted manually for control (A, bacteria suspension without sample) and BTAC-loaded nanofibrous membranes (B). Bacteria reduction was reported as percentage and  $\log_{10}$ . The

percentage reduction of bacteria (%) =  $(A - B)/A \times 100$ , and logarithm reduction =  $\log(A/B)$ .

To better understand the concept of prolonged release of drug in the core-shell nanofibers, we designed a separate antibacterial experiment against *S. aureus*. In this experiment, nanofibrous membranes CS 3.5 and S 3.5 were immersed in an 8 log bacterial suspension for 2 h. After 2 h, they were taken out, washed gently with PBS, and immersed in another fresh bacterial suspension at the same concentration (cfu/mL). We repeated this test for two more times and compared the antibacterial efficacy of core-shell and single nanofibrous membranes.

**4.6. Cytotoxicity Tests.** We applied an in vitro cytotoxicity assay of drug-loaded nanofibrous membranes against fibroblast cells (ATCC-PCS-201 neonatal human dermal fibroblast).<sup>29</sup> Nanofibrous membranes were cut into the same shape and weighed to 4 mg (triplicate). They were presoaked in 1 mL of ethanol for 10 min. Samples were then exposed to UV light for 45 min (each side). Fibroblast cells were cultured in 24 well plates at the density of  $1 \times 10^5$  (cell/mL). After 90% confluence was reached, 2 mL of fibroblast culture medium was added to each of the wells, and the nanofibrous membranes were added. Then, the cells were incubated at  $37^\circ\text{C}$  for 24 h. At the end of the incubation, cell viability was determined using the MTT assay after removal of membranes. Each well received 500  $\mu\text{L}$  of 1:10 (v/v) MTT and fibroblast medium solution. Subsequently, after 2 h incubation at  $37^\circ\text{C}$ , the media were aspirated and replaced by 500  $\mu\text{L}$  DMSO. Last, 100  $\mu\text{L}$  aliquots from each well (in triplicate) were transferred to a 96-well plate, and viability of cells was evaluated by recording the absorbance at 570 nm using a spectrophotometer (PowerWave XS2 Microplate Spectrophotometer, BioTek Instruments Inc., Canada).

**4.7. Statistical Analysis.** Statistical analyses were performed via PASW Statistics program package, version 18 (SPSS Inc., Chicago, IL, USA). Comparison of obtained data for different samples was performed using a one-way analysis of variance with Tukey's post-hoc test. The significance level was set at  $p < 0.05$ .

## ■ ASSOCIATED CONTENT

### 📄 Supporting Information

The Supporting Information is available free of charge on the ACS Publications website at DOI: 10.1021/acsomega.8b03137.

Cumulative release of BTAC from the single and core-shell nanofibers in TSB (PDF)

## ■ AUTHOR INFORMATION

### Corresponding Author

\*E-mail: Song.Liu@umanitoba.ca.

### ORCID

Song Liu: 0000-0003-0301-9535

### Present Address

<sup>†</sup>Chemical Engineering Department, Faculty of Engineering, McGill University, 3610 University Street, Montreal, QC, Canada, H3A 0C5.

### Notes

The authors declare no competing financial interest.

## ACKNOWLEDGMENTS

The authors acknowledge the financial support by a Collaborative Health Research Project (CHRP) operating grant (grant no. CHRP 413713-2012) and a Natural Sciences and Engineering Research Council of Canada (NSERC) Discovery grant (grant no. RGPIN/04922-2014). The authors also gratefully acknowledge the technical assistance of Mohammad Reza Kazemian in drawing the electrospinning scheme in Figure 1.

## REFERENCES

- (1) Augustine, R.; Kalarikkal, N.; Thomas, S. Electrospun PCL membranes incorporated with biosynthesized silver nanoparticles as antibacterial wound dressings. *Appl. Nanosci.* **2015**, *6*, 337–344.
- (2) Thet, N. T.; et al. Prototype Development of the Intelligent Hydrogel Wound Dressing and Its Efficacy in the Detection of Model Pathogenic Wound Biofilms. *ACS Appl. Mater. Interfaces* **2015**, *8*, 14909–14919.
- (3) Traba, C.; Liang, J. F. Bacteria responsive antibacterial surfaces for indwelling device infections. *J. Controlled Release* **2015**, *198*, 18–25.
- (4) Craig, M.; Amiri, M.; Holmberg, K. Bacterial protease triggered release of biocides from microspheres with an oily core. *Colloids Surf, B* **2015**, *127*, 200–205.
- (5) Xiong, M.-H.; Li, Y.-J.; Bao, Y.; Yang, X.-Z.; Hu, B. Bacteria-responsive multifunctional nanogel for targeted antibiotic delivery. *Adv. Mater.* **2012**, *24*, 6175.
- (6) Bean, J. E.; et al. Triggered release of Bacteriophage K from agarose/hyaluronan hydrogel matrixes by staphylococcus aureus virulence factors. *Chem. Mater.* **2014**, *26*, 7201–7208.
- (7) Tokiwa, Y.; Calabia, B.; Ugwu, C.; Aiba, S. Biodegradability of plastics. *Int. J. Mol. Sci.* **2009**, *10*, 3722–3742.
- (8) Xiong, M.-H.; et al. Lipase-Sensitive Polymeric Triple-Layered Nanogel for “On-Demand” Drug Delivery. *J. Am. Chem. Soc.* **2012**, *134*, 4355–4362.
- (9) Jiang, S.; et al. Efficient Nanofibrous Membranes for Antibacterial Wound Dressing and UV Protection. *ACS Appl. Mater. Interfaces* **2016**, *8*, 29915–29922.
- (10) Zahedi, P.; Rezaeian, I.; Ranaei-Siadat, S. O.; Jafari, S. H.; Supaphol, P. A review on wound dressings with an emphasis on electrospun nanofibrous polymeric bandages. *Polym. Adv. Technol.* **2010**, *21*, 77–95.
- (11) Dong, Y.; Liao, S.; Ngiam, M.; Chan, C. K.; Ramakrishna, S. Degradation Behaviors of Electrospun Resorbable Polyester Nanofibers. *Tissue Eng., Part B* **2009**, *15*, 333–351.
- (12) Cui, W.; Zhou, Y.; Chang, J. Electrospun nanofibrous materials for tissue engineering and drug delivery. *Sci. Technol. Adv. Mater.* **2010**, *11*, 014108.
- (13) Kim, G.-M.; et al. Electrospinning of PCL/PVP blends for tissue engineering scaffolds. *J. Mater. Sci.: Mater. Med.* **2013**, *24*, 1425–1442.
- (14) Hoang, K.-C.; Tseng, M.; Shu, W.-J. Degradation of polyethylene succinate (PES) by a new thermophilic Microbispora strain. *Biodegradation* **2006**, *18*, 333–342.
- (15) He, M.; Jiang, H.; Wang, R.; Xie, Y.; Zhao, C. Fabrication of metronidazole loaded poly( $\epsilon$ -caprolactone)/zein core/shell nanofiber membranes via coaxial electrospinning for guided tissue regeneration. *J. Colloid Interface Sci.* **2017**, *490*, 270–278.
- (16) Yang, Y.; et al. Promotion of skin regeneration in diabetic rats by electrospun core-sheath fibers loaded with basic fibroblast growth factor. *Biomaterials* **2011**, *32*, 4243–4254.
- (17) Elahi, M. F.; Lu, W.; Guoping, G.; Khan, F. Core-shell Fibers for Biomedical Applications-A Review. *J. Bioeng Biomed. Sci.* **2013**, *3*, 121.
- (18) Huang, Z.-M.; et al. Encapsulating drugs in biodegradable ultrafine fibers through co-axial electrospinning. *J. Biomed. Mater. Res., Part A* **2006**, *77A*, 169–179.
- (19) Zhang, Y.; Huang, Z.-M.; Xu, X.; Lim, C. T.; Ramakrishna, S. Preparation of Core-Shell Structured PCL-r-Gelatin Bi-Component Nanofibers by Coaxial Electrospinning. *Chem. Mater.* **2004**, *16*, 3406–3409.
- (20) Sun, Z.; Zussman, E.; Yarin, A. L.; Wendorff, J. H.; Greiner, A. Compound Core-Shell Polymer Nanofibers by Co-Electrospinning. *Adv. Mater.* **2003**, *15*, 1929–1932.
- (21) Irani, M.; Mir, G.; Sadeghi, M.; Haririan, I. Electrospun Biocompatible Poly( $\epsilon$ -caprolactonediol) Based Polyurethane Core/Shell Nanofibrous Scaffold for Controlled Release of Temozolomide. *Int. J. Polym. Mater. Polym. Biomater.* **2017**, *67*, 361.
- (22) Jones, E. M.; Cochrane, C. A.; Percival, S. L. The Effect of pH on the Extracellular Matrix and Biofilms. *Adv. Wound Care* **2015**, *4*, 431–439.
- (23) Jennings, M. C.; Minbiole, K. P. C.; Wuest, W. M. Quaternary Ammonium Compounds: An Antimicrobial Mainstay and Platform for Innovation to Address Bacterial Resistance. *ACS Infect. Dis.* **2016**, *1*, 288–303.
- (24) Ning, C.; et al. Enhanced antibacterial activity of new “composite” biocides with both N-chloramine and quaternary ammonium moieties. *RSC Adv.* **2015**, *5*, 93877–93887.
- (25) Nantel, G.; Proulx, P. Lipase activity in *E. coli*. *Biochim. Biophys. Acta, Lipids Lipid Metab.* **1973**, *316*, 156–161.
- (26) Paskiabi, F. A.; et al. Terbinafine-loaded wound dressing for chronic superficial fungal infections. *Mater. Sci. Eng. C* **2017**, *73*, 130–136.
- (27) Zhou, Y.; et al. Electrospun Water-Soluble Carboxyethyl Chitosan/Poly (vinyl alcohol) Nanofibrous Membrane as Potential Wound Dressing for Skin Regeneration. *Biomacromolecules* **2008**, *9*, 349–354.
- (28) Abdali, Z.; Yeganeh, H.; Solouk, A.; Gharibi, R.; Sorayya, M. Thermoresponsive antimicrobial wound dressings via simultaneous thiol-ene polymerization and in situ generation of silver nanoparticles. *RSC Adv.* **2015**, *5*, 66024–66036.
- (29) Asghari, S.; Logsetty, S.; Liu, S. Imparting commercial antimicrobial dressings with low-adherence to burn wounds. *Burns* **2016**, *42*, 877–883.